

Experimental nuclear-reaction studies and nuclear astrophysics¹⁾

E. Somorjai

Institute of Nuclear Research of the Hungarian Academy of Sciences, Debrecen, Hungary

Fiz. Elem. Chastits At. Yadra **23**, 974–992 (July–August 1992)

The main goal of the paper is to show the close relation between nuclear spectroscopy in nuclear reactions and nuclear astrophysics and to show that certain processes which are studied under normal conditions are enhanced in astrophysics.

1. INTRODUCTION

Nuclear astrophysics is a very prosperous and fast developing field. It is a combination of astrophysics and nuclear physics. It would take hours to mention only the most important parts of it. Therefore, in the brief time allotted here the subject should be strongly reduced. Namely, only low-energy charged-particle-induced nuclear reactions will be discussed here. However, it turns out that from the astrophysical point of view reactions of this kind (thermonuclear) are the most important ones. In stars they play the leading role as sources of energy and of element synthesis.

The main goal of my talk is—without entering into details of nuclear astrophysics—to show, on the one hand, the close relation between nuclear spectroscopy in nuclear reactions and nuclear astrophysics and, on the other hand, the significance of processes which are negligible under normal circumstances but important in astrophysics. That aim will be fulfilled by three examples. Two of them are experimental works (with my participation during a one-year study in Münster, Germany), and the third one (taken from Ref. 1) is a complex, expressive consequence of selection rules in nuclear physics. Before the examples, a very short introductory description of the synthesis of elements and star evolution is given together with a few basic relations in nuclear astrophysics.

The elemental abundances are the result of mixing in the course of a cyclic evolution shown in Fig. 1.² Some material can escape from the cycle as stellar residues (white dwarfs, etc.) or galactic cosmic-ray nuclei and, on the other hand, some material (possibly of Big Bang composition) may fall in. In the cycling process the stars are the very sites for different nuclear reactions providing energy for stabilizing themselves against gravitational contraction during the different burning stages (Fig. 2) of their life. A burning stage is also responsible for changes in elemental composition, while the intercurrent episodes of gravitational contraction (downward arrows in Fig. 2) generate temperature increases. The general evolution of a massive ($M=25M_{\odot}$) star is shown schematically in Fig. 2, taken from Ref. 3. The figure illustrates the central temperatures, densities, and duration of different burning stages with the most abundant nuclei left after a given burning mode. The figure also shows that a burning phase after its completion is drawn out from the central region into a thin peripheral shell, so that the deep stellar regions are similar to an onion with different skins of different

composition. The fate of a star is very complex (depending mostly on its mass), and a detailed treatment of that question is far beyond the scope of this talk.

All the critical stellar features (energy production, nucleosynthesis of elements, etc.) depend directly on the magnitude of the reaction rate per particle pair, $\langle\sigma v\rangle$:²

$$\langle\sigma v\rangle = \left(\frac{8}{\pi M_{12}}\right)^{1/2} \frac{1}{(kT)^{3/2}} \int_0^{\infty} \sigma(E) \exp\left(-\frac{E}{kT}\right) E dE, \quad (1)$$

where $\langle\sigma v\rangle$ means a value averaged over the velocity distribution, which is a Maxwell–Boltzmann one in the case of normal stellar gas (thermodynamic equilibrium). Here T refers to the temperature of the gas, M_{12} is the reduced mass of the interacting nuclei, $E=\frac{1}{2}M_{12}v^2$ is the center-of-mass energy, and $\sigma(E)$ is the reaction cross section. For nonresonant charged-particle-induced reactions the cross section can be expressed as

$$\sigma(E) = S(E) \frac{1}{E} \exp(-2\pi\eta), \quad (2)$$

(for details see, e.g., Ref. 2), where the function $S(E)$ defined here is referred to as the nuclear or astrophysical S factor containing all the strictly nuclear effects. The quantity η is called the Sommerfeld parameter, and $2\pi\eta$ is the Gamow factor expressing approximately the tunneling probability for particles with charges Z_1 and Z_2 :

$$2\pi\eta = 2\pi Z_1 Z_2 e^2 / \hbar v. \quad (3)$$

Combining Eqs. (1)–(3), the reaction rate per particle pair is

$$\langle\sigma v\rangle = \left(\frac{8}{\pi M_{12}}\right)^{1/2} \frac{1}{(kT)^{3/2}} \int_0^{\infty} S(E) \times \exp(-E/kT) \exp(-2\pi\eta) dE, \quad (4)$$

which is shown graphically in Fig. 3.² The product of the two exponential terms (hatched area) leads to a relatively narrow energy window around the effective burning energy of E_0 ($E_0 > kT$), where the nuclear reactions take place. In general, for stellar temperatures this window is far below the Coulomb barrier (e.g., $E_0=14.8$ keV for ${}^7\text{Li}+p$ at $T=15\times 10^6$ K and $E_{\text{Coul}}\cong 1.7$ MeV); consequently, the experimental reaction cross sections are needed at very low (essentially at zero) energies. [For resonance reactions Eq. (4) contains the sum of resonance strengths instead of the $S(E)$ factor.²] The cross section $\sigma(E)$ of a charged-particle-induced reaction drops sharply with decreasing en-

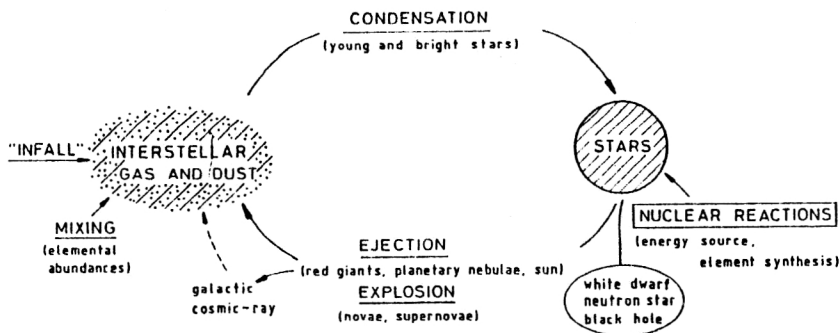


FIG. 1. Schematic picture of the material circulation in a galaxy.¹

ergy E for beam energies below the Coulomb barrier E_C , which means a practical lower limit E_L for cross-section measurements; thus, the only way is the extrapolation. Since the S factor is a smoothly varying function of energy, the advantage of using it instead of $\sigma(E)$ [Eq. (2)] is obvious, as is clearly demonstrated in Fig. 4.² Note the logarithmic and linear scales on the upper and lower parts of Fig. 4, respectively.

On the basis of the very short review above, one might come to the conclusion that only the reaction cross sections are needed for astrophysics. It is true, however, that for getting reliable cross-section data the full arsenal of nuclear spectroscopy has to be used. The above-sketched features of nuclear astrophysics are very simplified ones; the general case is shown in Fig. 5.² Besides the nonresonant case, there are other processes contributing to the S factor (or cross section), namely, resonances at higher energies

(broad ones) or at lower energies (sometimes in the extrapolation region) and even below the reaction threshold. In addition, interferences can frequently occur between resonant and nonresonant processes. To take all these phenomena into account an accurate knowledge of the reaction mechanism and resonances together with their parameters (J^π , strength, width, etc.) is necessary. For that, sometimes additional reaction(s) must be studied too (for resonances in the extrapolation and subthreshold region).

Before turning to the examples mentioned above it should be emphasized that besides the charged-particle-induced reactions discussed here, other reactions, like neutron capture, photodisintegration, and to some extent fusion of light heavy ions, are also very important in astrophysics. However, they are beyond the scope of this talk.

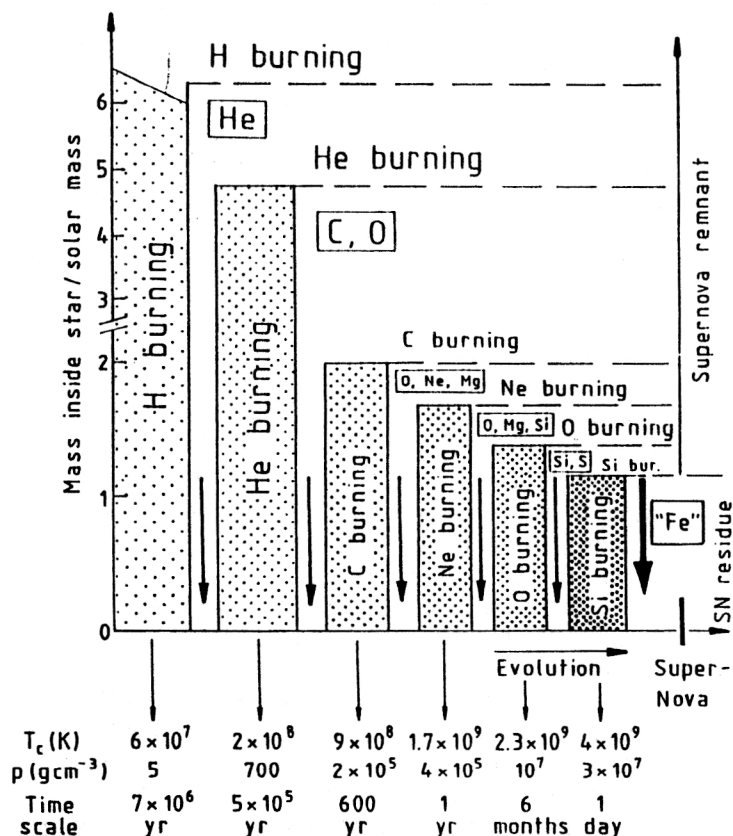


FIG. 2. General evolution (schematic) of a star with $M=25M_\odot$ (Ref. 3).

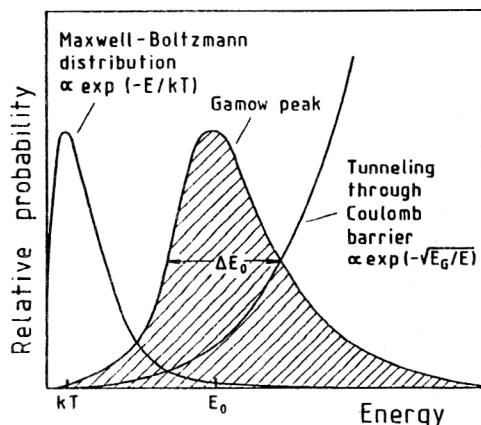


FIG. 3. Schematic diagram of the effective stellar energy region for nuclear reactions between charged particles.²

2. ELECTRON SCREENING IN THE REACTION

^{6,7}Li(*p*, α)^{3,4}He

As was pointed out in the previous section, to obtain the $S(E)$ value at the effective stellar energy (≈ 0) the experimental values must be extrapolated. To improve the extrapolated value, experimentalists make every effort to perform measurements at lower and lower energies. However, according to a prediction⁴ for the cross section of reactions between light nuclei and projectiles (mostly protons) at low energies, a simple process negligible at higher energies (electron screening) becomes significant. The basic idea of this screening is the following.

In nuclear physical treatments [e.g., Eqs. (2) and (3)] it is assumed that the Coulomb potential of the target nucleus as seen by the projectile is that resulting from a bare nucleus, and it would thus extend to infinity. However, for nuclear reactions studied in the laboratory the target nuclei are usually in the form of atoms or molecules. The atomic (or molecular) electron cloud surrounding the target nucleus acts as a screening potential: an incoming projectile

sees no repulsive Coulomb force until it penetrates beyond the atomic radius R_a ; thus, it effectively sees a reduced Coulomb barrier. At low projectile energies, when the classical turning point R_c of an incoming particle for the bare nucleus is near or outside the atomic radius, the magnitude of the shielding effect becomes significant: the condition $R_c \geq R_a$ leads to energies $E < U_e = Z_1 Z_2 e^2 / R_a$. Setting R_a equal to the radius of the innermost electrons of the target (or projectile) atoms, the resulting energies U_e are quite low [e.g., $U_e = 0.24$ keV for ⁷Li(*p*, α)⁴He], and thus the shielding effects might really appear to be effectively unimportant. However, the penetration through a shielded Coulomb barrier at energy E is equivalent to that of bare nuclei at energy $E_{\text{eff}} = E + U_e$. Thus, the shielding effect increases the cross section with an enhancement factor f given by⁴

$$f = \frac{\sigma(E_{\text{eff}})}{\sigma(E)} \approx \frac{E}{E_{\text{eff}}} \frac{\exp[-2\pi\eta(E_{\text{eff}})]}{\exp[-2\pi\eta(E)]}$$

$$\approx \exp\left(\frac{\pi\eta(E)U_e}{E}\right) \quad \text{for } U_e \ll E, \quad (5)$$

i.e., the factor f increases exponentially with decreasing energy. For energies $E/U_e \geq 1000$ the shielding effects are negligible [e.g., $f \approx 1.003$ for ⁷Li(*p*, α)⁴He]. However, at energies $E/U_e \leq 100$ the shielding effects cannot be disregarded [e.g., $f \approx 14.0$ and 1.09 at $E/U_e = 10$ and 100 , respectively, for ⁷Li(*p*, α)⁴He] and become important for the understanding of the low-energy data.

Several reactions involving light nuclides have been studied towards, and in some cases even below, the region $E/U_e = 100$ (Ref. 4 and references therein). However, the experimental errors for these low-energy data are too large to draw any meaningful conclusions. The first real experimental evidence of the electron screening was found in the reaction ³He(*d*,*p*)⁴He (Ref. 5), and most of the theoretical calculations⁵⁻⁸ underestimate the experimental data.

Here new experimental data are presented for the reaction ^{6,7}Li(*p*, α)^{3,4}He (Ref. 9). The reactions were studied at the 100-kV accelerator at the Ruhr Universität Bochum (Germany), which provided beams of H_1^+ , H_2^+ , and H_3^+ ions at energies $E_{\text{lab}} = 20$ to 100 keV with particle current up to 3 mA and at the 350-kV accelerator at the Universität Münster, which provided ⁶Li⁺ and ⁷Li⁺ ions at energies $E_{\text{lab}} = 77$ to 350 keV. Solid LiF targets on Ta backing and H₂ gas targets were used. The solid targets were fabricated with lithium of natural abundance and with lithium enriched to 99% in ⁶Li in the cases of ⁷Li and ⁶Li targets, respectively. The thickness of the solid targets (300 to 1000 $\mu\text{g}/\text{cm}^2$) was large enough to totally stop the incoming protons. During the course of the experiments the stability of the solid targets was checked periodically: no target deterioration was observed for bombarding times of more than a week. The proton beam passed through a Cu collimator and was focused into a profile of about 1.5 cm diameter on the target. The target was mounted at 90° with respect to the beam direction. Direct water cooling was applied to the target. A liquid-nitrogen (LN₂) cooled in-line Cu tube extended from the collimator to within 3 mm of the target. The tube near the target had appropriate

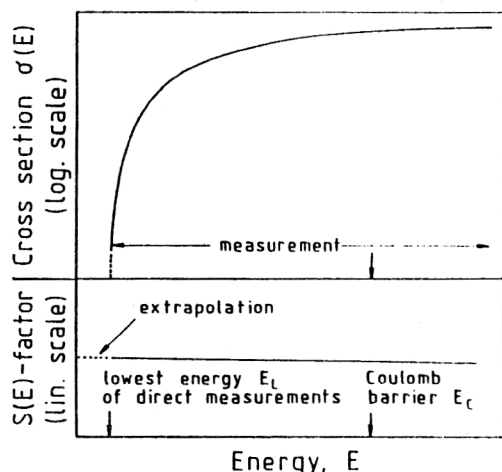


FIG. 4. The energy dependence of the cross section $\sigma(E)$ and the $S(E)$ factor for a charged-particle-induced nuclear reaction.²

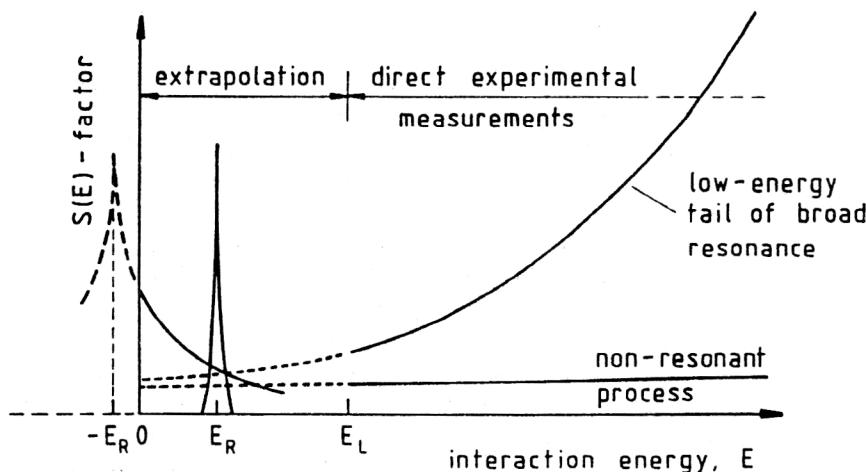


FIG. 5. The possible components of the $S(E)$ factor in charged-particle-induced reactions.²

holes to allow the observation of reaction products in four Si particle detectors (active area 450 and 600 mm², thickness 500 and 100 μ m) positioned at 130° with respect to the beam direction. A negative voltage of -300 V was applied to the tube to suppress secondary electrons from the target. The pressure in the target chamber was better than 2×10^{-6} mbar, and no carbon buildup on the target was observed.

For the reverse-reaction experiment a windowless gas target system of four pumping stages was used as a thin H₂ target. The beam entered the rectangular target chamber through five Ta apertures and was stopped in a 20-W beam calorimeter. The gas pressure in the chamber was measured with a Baratron capacitance manometer to an accuracy of better than $\pm 4\%$. The number of projectiles was measured via the calorimeter to an accuracy of $\pm 2.5\%$. Two Si detectors (active area 500 mm², thickness 2000 μ m) were installed in the chamber at opposite sides of the beam axis. Both in the solid-target and in the gas-target experiment, Ni foils were placed in front of the Si detectors to stop elastically scattered particles. In order to suppress the contribution of cosmic-ray events in the Si detectors, coincident signals from the Si detectors and a plastic scintillator (surrounding the target chamber) were rejected. Furthermore, a 5-cm thick lead shielding was placed around the plastic scintillator. Both in the solid and in the gas target cases these arrangements led to a reduction of the cosmic and room background by about a factor of 4.

The reaction yield $Y(E)$ obtained with infinitely thick targets is correlated with the cross section $\sigma(E)$,¹⁰ and with the $S(E)$ factor [Eq. (2)], by the relation

$$Y(E) = \int \sigma(E) \varepsilon^{-1} dE = \int S(E) E^{-1} \exp(-2\pi\eta) \varepsilon^{-1} dE, \quad (6)$$

where the integration is carried out from zero energy to the incident-beam energy, and ε is the stopping power.¹¹ The $S_{\text{BN}}(E)$ factor for the case of bare nuclei (BN) was obtained via a polynomial fit to the previous data at higher energies¹²⁻¹⁶ and an extrapolation down to the relevant energies of the present measurements (Fig. 6). The enhancement f is then given by the experimental yield (cor-

rected for the angular distribution and target stoichiometry), divided by the theoretical yield $Y_{\text{BN}}(E)$, obtained with the derived function $S_{\text{BN}}(E)$. The ratio was normalized to unity at the higher energies, where no screening effects are expected. Thus, the experimental $S(E)$ factor was determined by using the relation

$$S(E) = \int S_{\text{BN}}(E) = [Y(E)/Y_{\text{BN}}(E)] S_{\text{BN}}(E) \quad (7)$$

and is shown in Fig. 6. A fit to the data using Eq. (5) leads to screening potentials $U_e = 410 \pm 40$ eV and 400 ± 40 eV in the cases of ${}^7\text{Li}(p, \alpha){}^4\text{He}$ and ${}^6\text{Li}(p, \alpha){}^3\text{He}$, respectively. The values are significantly higher than the expected value⁴ quoted above (240 eV).

In the case of the thin H₂ gas target the corrections due to the infinitely thick targets can be avoided; otherwise, the $S(E)$ values were obtained as in the solid-target case. A fit to the data using Eq. (5) leads to screening potentials $U_e = 310 \pm 20$ eV for ${}^7\text{Li}(p, \alpha){}^4\text{He}$ and $U_e = 300 \pm 20$ eV for ${}^6\text{Li}(p, \alpha){}^3\text{He}$ (Fig. 7). The values are again higher than expected.

Since the electron cloud in the H₂ molecule (gas target) is at larger distances than in the H atom (projectile), the screening effect should be shifted to lower energies, i.e., $U_e(\text{H}_2 + \text{Li}) < U_e(\text{H} + \text{Li})$, as is shown qualitatively by our experimental values. A recent theoretical calculation⁸ strongly underestimates ($U_{\text{max}} = 186$ eV) the experimental values.

In summary, a good understanding of the screening effect requires additional efforts in the theory as well as in experimental work, i.e., one needs improved low-energy data for other fusion reactions. Such a program is in progress at the Ruhr Universität, Bochum.

3. NUCLEAR REACTION ON A RADIOACTIVE TARGET: ${}^{22}\text{Na}(p, \gamma){}^{23}\text{Mg}$

The main motivation of this experiment is related to the so-called Ne-E (E for extraordinary) problem, i.e., the discovery of neon remarkably enriched in ${}^{22}\text{Ne}$ with ${}^{22}\text{Ne}/{}^{20}\text{Ne} > 0.67$ (terrestrial ratio 0.1) in the Orgueuil meteorite.¹⁸ The results of subsequent refined

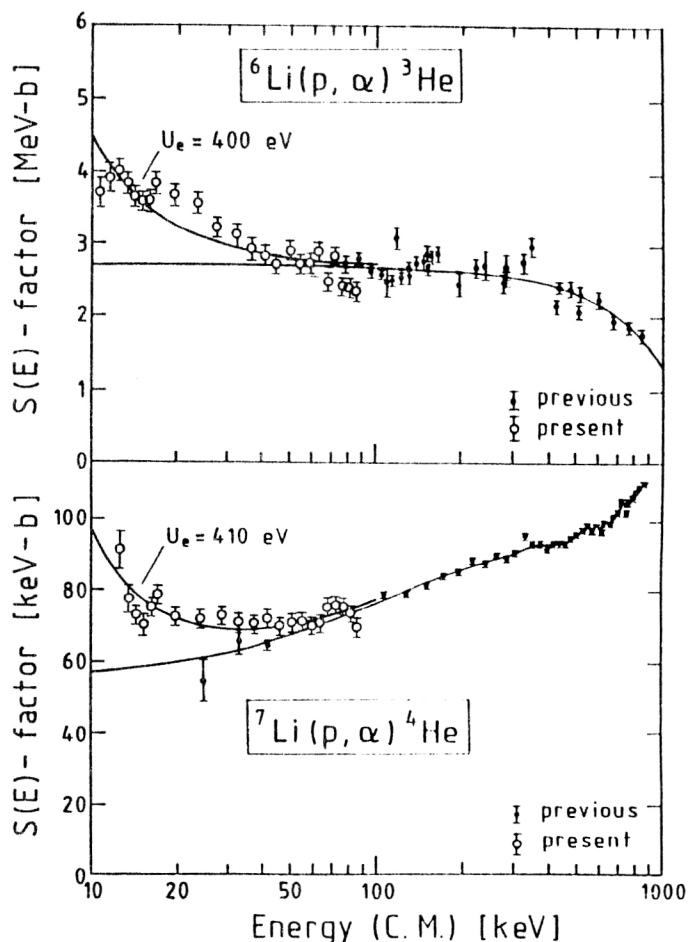


FIG. 6. The $S(E)$ -factor data for the solid-target cases. The lower curves are obtained from a fit to previous data at higher energies (see the text) and are assumed to represent the case of bare nuclei. The upper curves are the calculated enhancements using Eq. (5) with the fitted potentials shown in the figures.

measurements^{19,20} and detailed nucleosynthesis calculations^{21–23} have shown that the Ne–E is essentially fossil material of extinct ^{22}Na , and the hot NeNa cycle (Fig. 8) developing in explosive H-burning locations, and in particular in novae, could account for a sizable ^{22}Na production. However, recent calculations^{24,25} have predicted much lower ^{22}Na nova yields. This is due to a large increase in the calculated reaction rates for $^{22}\text{Na}(p,\gamma)^{23}\text{Mg}$, which is the key reaction for ^{22}Na destruction in the hot NeNa chain.² The experimental work discussed below¹⁷ gives a reevaluation of the rate of this important reaction in a range of energies (temperatures) that encompasses the most likely conditions of operation of the cold and hot NeNa chains of reactions.

The $^{22}\text{Na}(p,\gamma)^{23}\text{Mg}$ reaction is one of the examples of nuclear reactions induced on radioactive nuclei, the importance of which in the hot and explosive burning phases of stellar evolution has been addressed in recent years (Ref. 26).²⁾ It is shown in Fig. 8, where the dominant stable nuclei involved in the “cold”. (low-temperature) operation of the cycle are shaded. At higher temperatures, the nuclear burning times can become shorter than the half-lives; with increasing temperature the longer-lived ^{22}Na nuclides [and so the $^{22}\text{Na}(p,\gamma)^{23}\text{Mg}$ reaction] are the first to become relevant, and the cycle is said to operate in the “hot” mode. The next nucleus is ^{21}Na , and so on.

The experimental examination of the $^{22}\text{Na}(p,\gamma)^{23}\text{Mg}$

reaction—in addition to the already mentioned general experimental difficulties in nuclear astrophysics (low energy, small cross section)—requires a radioactive ^{22}Na target and the detection of capture gamma rays in the presence of the “hot” target. The level diagram of the reaction is shown in Fig. 9. In a previous experiment²⁷ only upper limits on the strengths of potential resonances were reported at $E_p^{\text{lab}} = 0.40\text{--}1.27$ MeV. Using improved experimental techniques, such as ^{22}Na mass-separator implanted targets (ISOLDE-II at CERN) and a threshold gamma-ray detector, the wide range of nuclear spectroscopy was performed for getting the necessary stellar reaction rates. For the experiment the 450-kV Sames accelerator and the 4-MV Dynamitron tandem accelerator at the Ruhr Universität Bochum provided proton beams up to $80\ \mu\text{A}$ on the target in the energy range $E_p = 0.17\text{--}1.29$ MeV. The beams from each accelerator were guided into the same target beam line. The beam passed through a long (1.08 m) LN_2 -cooled Cu shroud with a collimator at the end of it, an electrically insulated Cu disk (with a central hole), and was finally stopped at the target. A voltage of -300 V applied to the disk was sufficient for secondary-electron suppression from both the shroud and the target. Thus, the end of the beam pipe (electrically insulated, 70 cm long) together with the target formed a Faraday cup for beam integration. The targets were oriented perpendicular to the

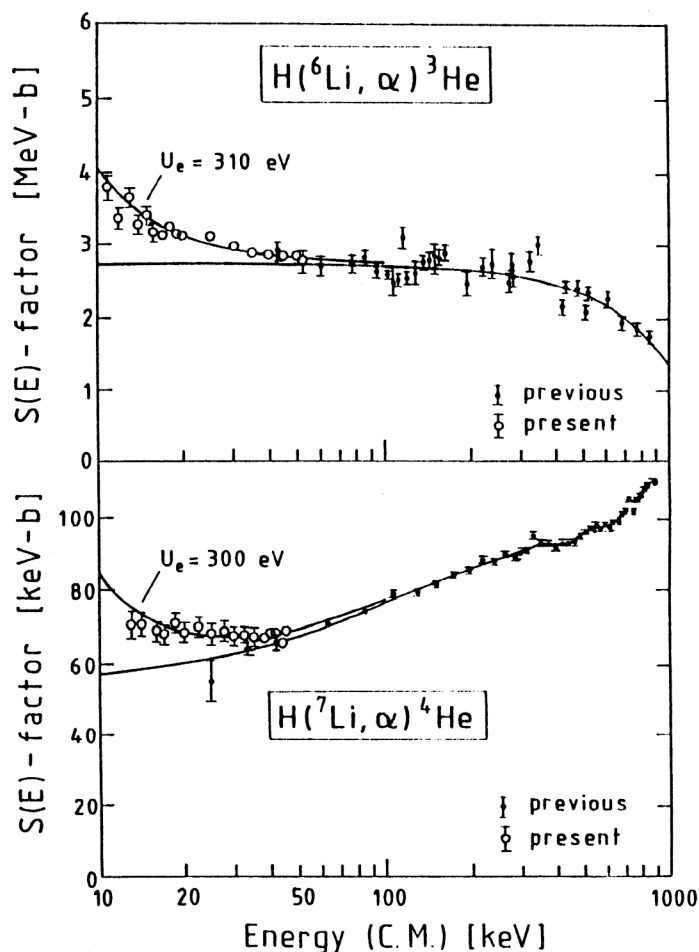


FIG. 7. The same as in Fig. 6, for the gas target.

beam direction. The effective mean diameter of the beam spot was about 5 mm. In order to minimize beam-induced gamma-ray background from the shroud collimator, its beam-facing side was coated with a Ni layer. The target substrates were directly water-cooled. With the LN₂-cooled Cu shroud (pressure near the target $\approx 2 \times 10^{-7}$ Torr) carbon deposition on the targets was

strongly reduced. The implanted target of 0.7 m Ci ²²Na activity was in the form of a Ni-Ta sandwich. The effective target thickness was 9 ± 1 keV at $E_p = 613$ keV.

Three different gamma-ray detectors have been used: a 7.6-cm $\varnothing \times 7.6$ -cm NaI(Tl) crystal, a 145-cm³ intrinsic Ge detector, and a threshold detector of 242 l D₂O (Ref. 28). The target and the NaI crystal were installed inside a cy-

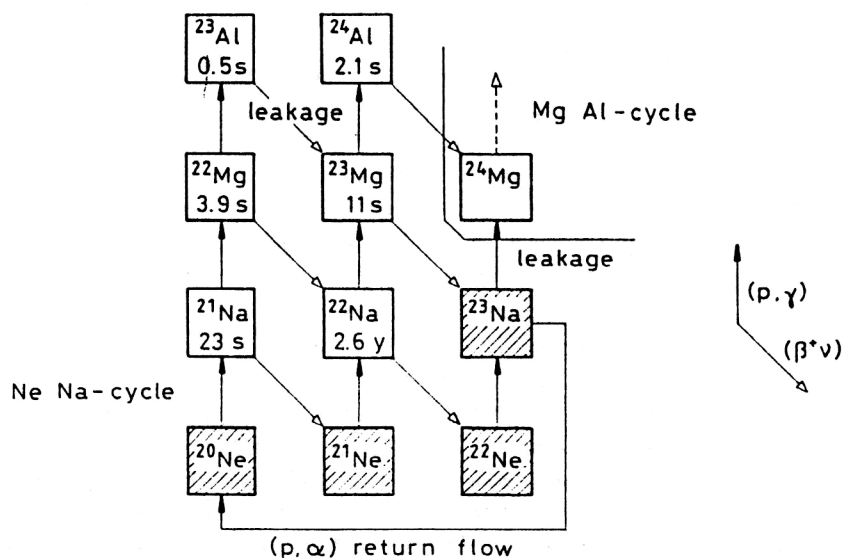
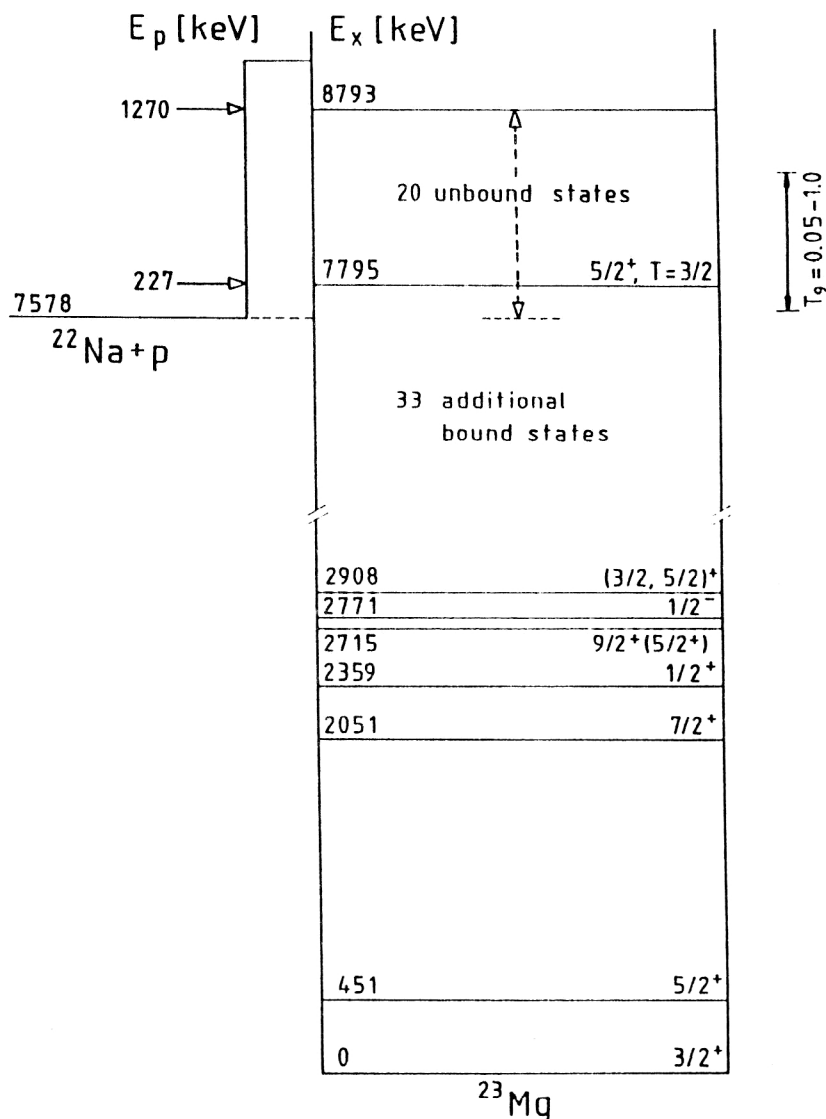


FIG. 8. The sequence of nuclear reactions and β decays in the hydrogen-burning NeNa cycle. The half-lives of the radioactive nuclides are indicated.



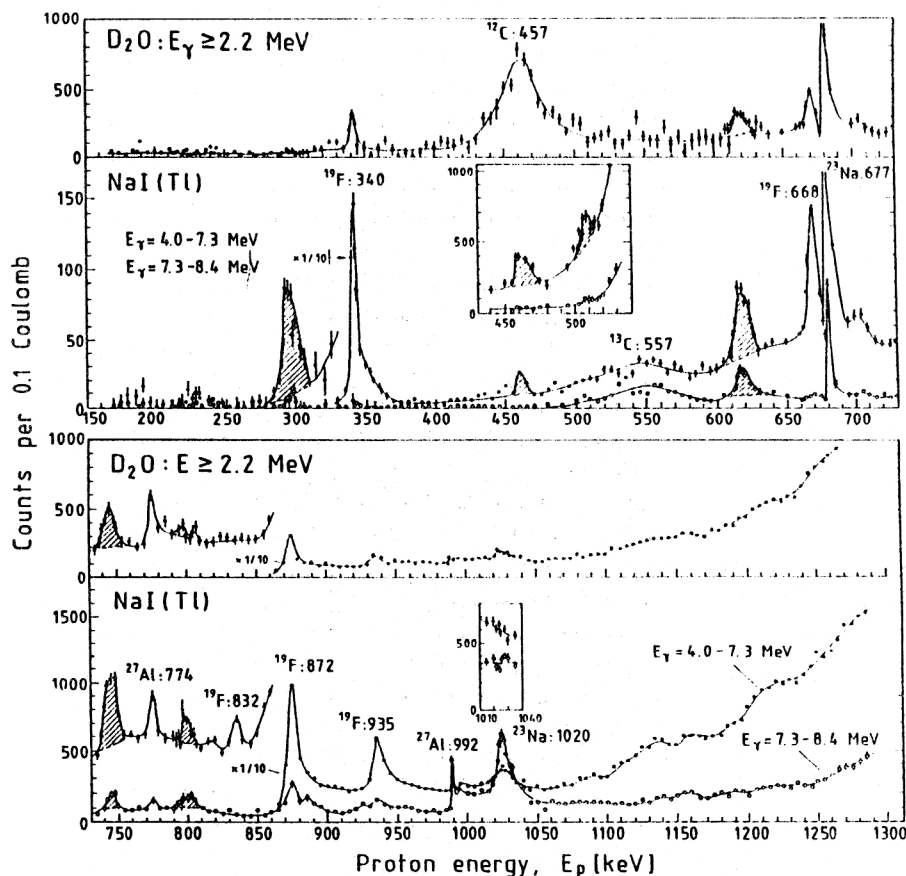


FIG. 10. Excitation functions of the reaction $^{22}\text{Na}(p,\gamma)^{23}\text{Mg}$. The energy windows and detectors are indicated. The insets show the functions taken after the bombardment with charge of 100 °C. The newly found resonances are shown by shaded structures. The curves through the data points are to guide the eyes only.

essentially blocking nucleosynthesis via He burning beyond ^{16}O .

As a consequence, the major ashes of He burning in red giants are carbon and oxygen, and it is generally be-

lieved that the ^{12}C and ^{16}O in galactic matter had their origin in these red giants. Both elements are also essential for the evolution of life; and it is only through some fortuitous nuclear properties and selection rules that both elements were produced so plentifully and survived the red-giant phase of stellar evolution. It is perhaps instructive to speculate on how our life and the universe as a whole might have looked if the mass of ^8Be had not been close to the mass of two alpha particles, if there was no enhancing resonant state in ^{12}C , or if there were no parity and isospin conservation laws. Einstein is quoted as saying, "God does not throw dice." This has not been verified one way or the other; but if He (or "She") does, She (or He) is incredibly lucky.

5. SUMMARY

Here an attempt has been made to show one of the main requirements of nuclear astrophysics, viz., many-sided knowledge of a large variety of nuclear reactions. For astrophysics many nuclear reactions or processes are important in the energy range from a few keV (thermonuclear reactions) up to about 100 MeV (spallation reactions); however, low-energy charged-particle-induced reactions—the subject of this review—are playing a key role in the evolution of stars producing energy and are mostly responsible for elemental nucleosynthesis.

The given examples (Secs. 2–4) hopefully have proved the importance of the precise knowledge of nuclear levels (bound or resonance ones), their parameters (J^π , T , Γ ,

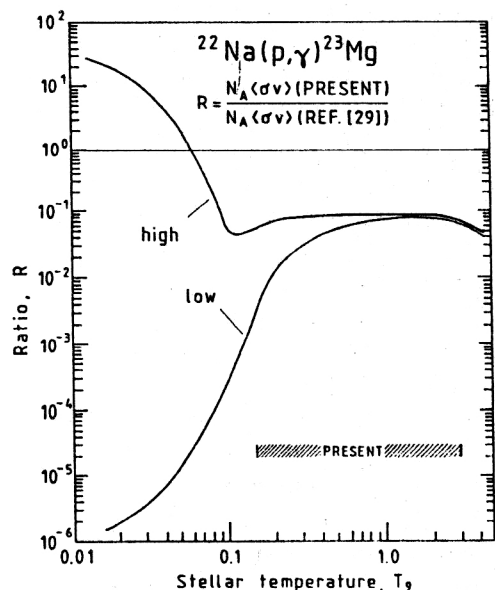


FIG. 11. Ratio of the present and previous²⁹ stellar reaction rates as a function of temperature. The curves labeled LOW and HIGH represent the values taken from the known resonance strengths only and from all potentially possible contributions, respectively.

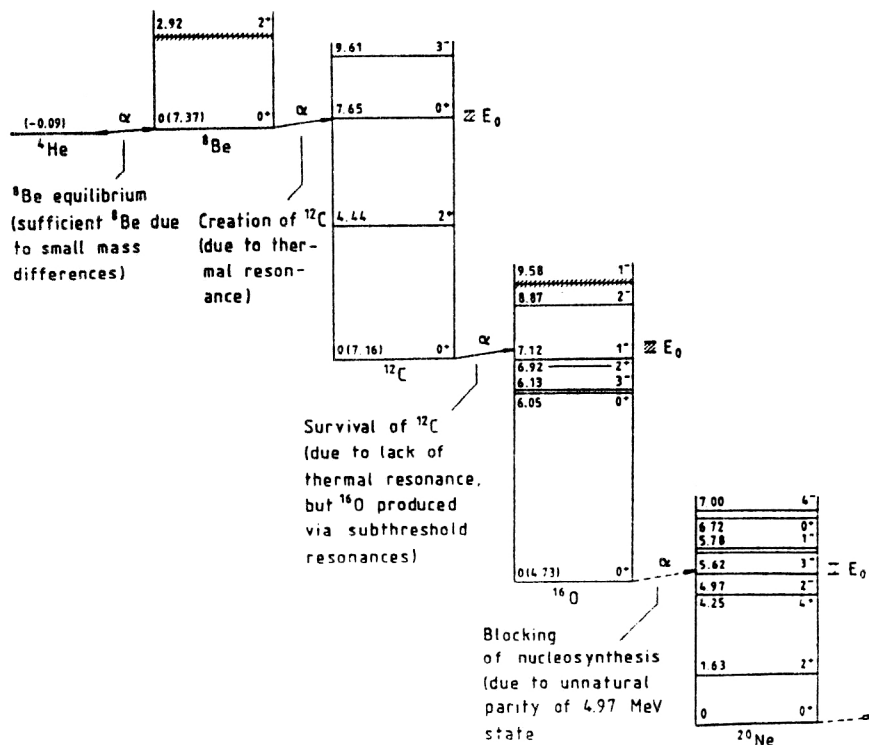


FIG. 12. Level schemes of nuclei involved in the He-burning reactions in red giants.¹ The effective stellar energies (E_0) are indicated.

$\omega\gamma$, etc.), and the reaction mechanism. It was perhaps interesting to show how the evolution of life is determined by conservation laws of nuclear physics.

One should never forget that, because of the nature of the astrophysical problems, there are many special requirements (e.g., experiments at very low energies) and processes (e.g., electron screening) which are not encountered in ordinary nuclear physics. Thus, nuclear astrophysics is a great challenge for experimentalists: somehow the extreme circumstances (temperature, density, etc.) of astrophysical sites have to be transported to the laboratory or must at least be simulated. Therefore it is often a frustrating science. The desired cross sections are among the smallest ones measured in the nuclear laboratory, requiring long measuring times with scrupulous attention to the background.

Last but not least, I would like to emphasize that nuclear astrophysics, in addition to the fact that it is a fast developing discipline, has also originated extremely active new fields, like experiments on "hot" targets or by "hot" beams (see, e.g., Ref. 2 and references therein).

Thanks are due to C. Rolfs (Bochum) for his invitation to take part in the astrophysical experiments reported here and for excellent hospitality during that period.

¹Talk given at the session "Trends in Physics" at the Hungarian Academy of Sciences (7 May 1991).

²It should be noted that radioactive beams have the same importance with only a practical difference, i.e., for nuclei with half-life $T_{1/2} < 1$ h radioactive-beam experiments, and for $T_{1/2} > 1$ h radioactive-target experiments, are more advantageous.²

¹C. Rolfs, H. P. Trautvetter, and W. S. Rodney, Rep. Prog. Phys. **50**, 233 (1987).

²C. Rolfs and W. S. Rodney, *Cauldrons in the Cosmos* (University of Chicago Press, Chicago, 1988).

³M. Arnould and M. Rayet, Ann. Phys. Fr. **15**, 183 (1990).

⁴H. J. Assenbaum, K. Langanke, and C. Rolfs, Z. Phys. A **327**, 461 (1987).

⁵S. Engstler et al., Phys. Lett. **202B**, 179 (1988).

⁶Gy. Bencze, Nucl. Phys. **A492**, 459 (1989).

⁷G. Bluge et al., Z. Phys. A **333**, 219 (1989).

⁸L. Bracci et al., Nucl. Phys. **A513**, 316 (1990).

⁹U. Schroder et al., Nucl. Instrum. Methods **B40/41**, 466 (1989).

¹⁰H. E. Gove, in *Nuclear Reactions*, edited by P. M. Endt and P. B. Smith (North-Holland, Amsterdam, 1959), Vol. 1, p. 259.

¹¹H. H. Andersen and J. F. Ziegler, *Hydrogen—Stopping Powers and Ranges in All Elements* (Pergamon Press, New York, 1977).

¹²C. Rolfs and R. W. Kavanagh, Nucl. Phys. **A455**, 179 (1986).

¹³W. Gemeinhardt, D. Kamke, and C. Rhoneck, Z. Phys. **197**, 58 (1966).

¹⁴H. Spinka, T. A. Tombrello, and H. Winkler, Nucl. Phys. **A164**, 1 (1971).

¹⁵A. J. Elwyn et al., Phys. Rev. C **20**, 1984 (1979).

¹⁶T. Shinozuka, Y. Tanaka, and K. Sugiyama, Nucl. Phys. **A326**, 47 (1979).

¹⁷S. Seuthe et al., Nucl. Phys. **A514**, 471 (1990).

¹⁸D. C. Black, Geochim. Cosmochim. Acta **36**, 347 (1972).

¹⁹M. H. A. Jungck and P. Eberhardt, Meteoritics **14**, 439 (1979).

²⁰P. Eberhardt et al., Geochim. Cosmochim. Acta **45**, 1515 (1981).

²¹M. Arnould and W. Beelen, Astron. Astrophys. **33**, 215 (1974).

²²M. Arnould and H. Norgaard, Astron. Astrophys. **64**, 195 (1978).

²³D. D. Clayton and F. Hoyle, Astrophys. J. **203**, 490 (1976).

²⁴S. E. Woosley, in *Nucleosynthesis and Chemical Evolution*, edited by B. Hauck, A. Maeder, and G. Meynet (Observatoire de Geneva, 1986), p. 1.

²⁵M. Wiescher et al., Astron. Astrophys. **160**, 56 (1986).

²⁶W. A. Fowler, Rev. Mod. Phys. **56**, 149 (1984).

²⁷M. Wiescher et al., Nucl. Instrum. Methods **A267**, 242 (1988).

²⁸S. Seuthe et al., Nucl. Instrum. Methods **A272**, 814 (1988).

²⁹W. Wiescher and K. Langanke, Z. Phys. A **325**, 309 (1986).

Translated by the author